

Phase Diagrams of Mixed Spin Chains with Period 4 by the Nonlinear σ Model

Ken'ichi Takano

Laboratory of Theoretical Condensed Matter Physics and
Research Center for Advanced Photon Technology,
Toyota Technological Institute, Nagoya 468-8511, Japan

(Received)

We study mixed quantum spin chains consisting of two kinds of spins with magnitudes, s_a and s_b . The spins are arrayed as $s_a-s_a-s_b-s_b$ in a unit cell and the exchange couplings are accordingly periodic with period 4. The spin Hamiltonian is mapped onto a nonlinear σ model based on the general formula for periodic inhomogeneous spin chains. The gapless condition given by the nonlinear σ model determines boundaries between disordered phases in the space of the exchange parameters. The phase diagram has a rich phase structure characterized by the values of s_a and s_b . We explain all phases in the singlet-cluster-solid picture which is an extension of the valence-bond-solid picture.

PACS numbers: 75.10.Jm, 75.30.Et, 75.30.Kz

I. INTRODUCTION

Quantum spin systems have been investigated for long time and have revealed quantum states which do not appear in the corresponding classical systems. They have rich content as quantum many-body systems, although they are described by Hamiltonians much simpler than itinerant electron systems. Among spin systems the spin chain is especially interesting because quantum fluctuation is the largest in one dimension. For the last two decades, one of the most exciting discoveries in the spin chain is the Haldane gap. That is, a homogeneous antiferromagnetic spin chain is gapful if the spin magnitude is an integer, and is gapless if it is a half-odd integer. Haldane proposed this prediction based on the mapping of a spin chain onto the nonlinear σ model (NLSM) in a semiclassical manner [1]. Since then, the NLSM is strongly recognized to be important in research of quantum spin systems. Various interesting aspects of the NLSM method for spin chains are found in Refs. [2–4].

Affleck reformulated the NLSM method in an operator formalism [5]. He divided a spin chain into spin pairs and transformed the spin operators for each spin pair into operators representing an antiferromagnetic motion and a small fluctuation. The NLSM is analyzed by the field theoretic method [6]. It is important that his operator formalism is applicable even to a spin chain with bond alternation. The spin chain with spin magnitude $\frac{1}{2}$ has a finite spin gap if the bond alternation is finite. In this case, the ground state is in a dimer phase. A gapless spin excitation can appear only at the phase boundary between dimerized phases, where the system has no bond alternation. In contrast, a spin chain with spin magnitude 1 has a gapless spin excitation at a finite strength of the bond alternation. These results consist with those of numerical calculations [7,8] and with experimental results [9].

The bond alternation is the simplest inhomogeneity for the exchange parameter; the spin chain with bond alter-

nation is a system with period 2. The next interest is in inhomogeneous spin chains with periods more than 2. In general we can consider two kinds of inhomogeneities in a spin chain: one is for the exchange parameter and the other is for the spin magnitude. It is difficult to extend the operator formalism of Affleck to various inhomogeneous cases, since a very complicated transformation among operators may be needed. In particular, the difficulty is serious for mixed spin chains, where the spin magnitude is inhomogeneous.

In a previous paper, we unambiguously derived the NLSM for the general mixed spin chain with finite period [10]. The derivation is based on dividing the spin chain into blocks in a path integral formalism. Each block is a single unit cell or consists of a series of unit cells. A spin pair used by Affleck [5] can be regarded as an especially simple block containing only two spins. We carried out a transformation for spin variables in each block so as to preserve the original degrees of freedom. We finally obtained the NLSM action describing low energy behavior of the original spin chain [11]. The topological angle in the topological term of the NLSM depends on the exchange parameters and the magnitudes of spins, and determines whether or not the system has a gapless spin excitation. The gapless condition is given in a closed equation form; i. e. the *gapless equation*. This gapless equation is quite general, and is applicable to various spin chains.

In this paper, we present and examine the phase diagrams of spin chains with period 4 by means of the NLSM. We restrict ourselves to the case that two kinds of spins, s_a and s_b , compose a spin chain. The condition that the ground state is singlet allows only the array of $s_a-s_a-s_b-s_b$ in a unit cell. We apply the general NLSM method to the spin chain with period 4 and write down the gapless equation. The gapless equation determines gapless phase boundaries and hence the phase diagram for each pair of s_a and s_b . The phase diagram generally consists of many phases when s_a and/or s_b are large. To understand these phases, we introduce the singlet-

cluster-solid (SCS) picture. It is an extension of the valence-bond-solid (VBS) picture [12] and its special versions have been used (e. g. Refs. [13,14]). The SCS picture systematically explains all phases for any values of s_a and s_b .

This paper is organized as follows. In Sec. II, we introduce the general Hamiltonian for spin chains with period 4 and with singlet ground state. In Sec. III, the NLSM for the general spin chain with any period is reviewed. The gapless equation determined by the topological term is written. In Sec. IV, the general gapless equation is specialized to the period-4 case and its properties are mentioned. In Sec. V, the case of homogeneous spin magnitudes ($s_a=s_b$) is examined. Phase diagrams are obtained and explained in the SCS picture. In Sec. VI, the phase diagram is examined in the general case ($s_a<s_b$) and is interpreted in the SCS picture. Section VII is devoted to summary and discussion.

II. MIXED SPIN CHAIN WITH PERIOD 4

The Hamiltonian with period 4 is generally written as

$$H = \sum_{j=1}^{N/4} (J_1 \mathbf{S}_{4j+1} \cdot \mathbf{S}_{4j+2} + J_2 \mathbf{S}_{4j+2} \cdot \mathbf{S}_{4j+3} + J_3 \mathbf{S}_{4j+3} \cdot \mathbf{S}_{4j+4} + J_4 \mathbf{S}_{4j+4} \cdot \mathbf{S}_{4j+5}), \quad (1)$$

where \mathbf{S}_j is the spin at site j with magnitude s_j . The number of lattice sites is N , the lattice spacing is a and the system size is $L = aN$. We only consider the antiferromagnetic exchange interaction ($J_i > 0$). Since the system is periodic with period 4 in the spin magnitude as well as in the exchange parameter, we generally have 4 different spin magnitudes: s_1, s_2, s_3 and s_4 in a unit cell. However we concentrate systems with singlet ground states. Following the Lieb-Mattis theorem [15], a singlet ground state is realized if the system satisfies the condition

$$s_1 - s_2 + s_3 - s_4 = 0; \quad (2)$$

otherwise the system has a ferrimagnetic ground state.

We treat the case that two kinds of spins are mixed and denote the magnitudes as s_a and s_b . To consist with the restriction (2), the spin magnitudes in the j th unit cell are taken as

$$\begin{aligned} s_a &\equiv s_{4j+1} = s_{4j+2}, \\ s_b &\equiv s_{4j+3} = s_{4j+4} \quad (s_a \leq s_b) \end{aligned} \quad (3)$$

without further loss of generality. Correspondingly, we take the exchange parameters as

$$J_{aa} \equiv J_1, \quad J_{ab} \equiv J_2 = J_4, \quad J_{bb} \equiv J_3. \quad (4)$$

We often use the unit of $J_{bb}(=J_3) = 1$. A unit cell of the lattice is illustrated in Fig. 1.

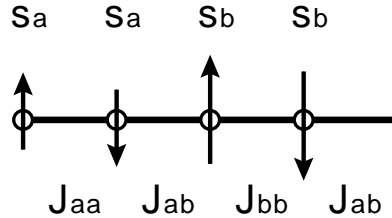


FIG. 1. Spin magnitudes and exchange parameters in a unit cell of the Hamiltonian (1) with Eqs. (3) and (4).

III. NLSM FOR THE GENERAL SPIN CHAIN

In this section we summarize the essential results in Ref. [10], in which the NLSM is derived for the general spin chain with arbitrary period. The Hamiltonian examined in Ref. [10] is

$$H = \sum_{j=1}^N J_j \mathbf{S}_j \cdot \mathbf{S}_{j+1} \quad (5)$$

with

$$J_{j+2b} = J_j, \quad s_{j+2b} = s_j, \quad (6)$$

where b is a positive integer. We consider the spin chain by dividing it into blocks of size $2b$. The period $2b$ need not be a unit cell, but it may be a positive integer multiple of a unit cell [16]. In order that the mapping of the Hamiltonian (5) to the NLSM is successfully carried out, the spin magnitudes must satisfy the restriction

$$\sum_{j=1}^{2b} (-1)^j s_j = 0. \quad (7)$$

The restriction coincides with the condition (2), which excludes the ferrimagnetic ground state.

The expectation value of a spin operator in a coherent state is expressed as

$$\langle \mathbf{S}_j \rangle = (-1)^j s_j \mathbf{n}_j \quad (8)$$

with a unit vector \mathbf{n}_j . The partition function Z at temperature $1/\beta$ is then represented as

$$Z = \int D[\mathbf{n}_j] \prod_j \delta(\mathbf{n}_j^2 - 1) e^{-S}, \quad (9)$$

$$\begin{aligned} S &= i \sum_{j=1}^N (-1)^j s_j w[\mathbf{n}_j] \\ &+ \int_0^\beta d\tau \sum_{j=1}^N J_j s_j s_{j+1} \mathbf{n}_j \cdot \mathbf{n}_{j+1}. \end{aligned} \quad (10)$$

In the action (10), the first term comes from the Berry phase and $w[\mathbf{n}_j]$ is the solid angle which the unit vector \mathbf{n}_j forms in the period β .

We transform the spin variables $\{\mathbf{n}_j\}$ into gradually changing unit vectors $\{\mathbf{m}(p)\}$ and their small fluctuations $\{\mathbf{L}_q(p)\}$. The spin variable at the q th site in the p th block is written as

$$\mathbf{n}_{2bp+q} = (1 - z_q)\mathbf{m}(p) + z_q\mathbf{m}(p - \gamma_q) + a\mathbf{L}_q(p) \quad (11)$$

with $z_q = |b - q|/2b$ and $\gamma_q = \text{sgn}(b - q)$. This transformation does not change the number of the original degrees of freedom as is explained in Ref. [10]. Integrating out the fluctuations and taking the continuum limit, we finally obtain the effective action [10]:

$$S_{\text{eff}} = \int_0^\beta d\tau \int_0^L dx \left\{ -i \frac{J^{(0)}}{J^{(1)}} \mathbf{m} \cdot (\partial_\tau \mathbf{m} \times \partial_x \mathbf{m}) + \frac{1}{2aJ^{(1)}} \left(\frac{J^{(1)}}{J^{(2)}} - \frac{J^{(0)}}{J^{(1)}} \right) (\partial_\tau \mathbf{m})^2 + \frac{a}{2} J^{(0)} (\partial_x \mathbf{m})^2 \right\}, \quad (12)$$

where $J^{(n)}$ ($n = 0, 1, 2$) is defined as

$$\frac{1}{J^{(n)}} = \frac{1}{2b} \sum_{q=1}^{2b} \frac{(\tilde{s}_q)^n}{J_q s_q s_{q+1}}, \quad (13)$$

$$\tilde{s}_q = \sum_{k=1}^q (-1)^{k+1} s_k. \quad (14)$$

The action (12) is of the standard form of the NLSM:

$$S_{\text{st}} = \int_0^\beta d\tau \int_0^L dx \left\{ -i \frac{\theta}{4\pi} \mathbf{m} \cdot (\partial_\tau \mathbf{m} \times \partial_x \mathbf{m}) + \frac{1}{2gv} (\partial_\tau \mathbf{m})^2 + \frac{v}{2g} (\partial_x \mathbf{m})^2 \right\}, \quad (15)$$

where θ is the topological angle, g is the coupling constant and v is the spin wave velocity.

The NLSM has a gapless excitation when $\theta/2\pi$ is a half-odd integer. Comparing Eq. (12) and Eq. (15), this condition is written in the gapless equation:

$$\frac{1}{J^{(1)}} = \frac{2l - 1}{4} \frac{1}{J^{(0)}}, \quad (16)$$

where l is an arbitrary integer. For each l , this equation determines a boundary between disordered phases if it has a solution. Note that Eq. (16) is linear in $\{1/J_j\}$.

IV. GAPLESS LINES FOR THE SPIN CHAIN WITH PERIOD 4

In the present case of Eqs. (3) and (4), the transformation (11) is explicitly written as

$$\mathbf{n}_{4p+1} = \frac{3}{4}\mathbf{m}(p) + \frac{1}{4}\mathbf{m}(p-1) + a\mathbf{L}_1(p), \quad (17)$$

$$\mathbf{n}_{4p+2} = \mathbf{m}(p) + a\mathbf{L}_2(p), \quad (18)$$

$$\mathbf{n}_{4p+3} = \frac{3}{4}\mathbf{m}(p) + \frac{1}{4}\mathbf{m}(p+1) + a\mathbf{L}_3(p), \quad (19)$$

$$\mathbf{n}_{4p+4} = \frac{1}{2}\mathbf{m}(p) + \frac{1}{2}\mathbf{m}(p+1) + a\mathbf{L}_4(p) \quad (20)$$

for the p th block. Note that $\mathbf{m}(p-1)$ and $\mathbf{m}(p+1)$ are variables belonging to the neighboring blocks. Since Eq. (14) is reduced to

$$\tilde{s}_1 = s_a, \quad \tilde{s}_3 = s_b, \quad \tilde{s}_2 = \tilde{s}_4 = 0, \quad (21)$$

then Eq. (13) yields

$$\frac{1}{J^{(0)}} = \frac{1}{4} \left(\frac{1}{J_{aa}s_a^2} + \frac{2}{J_{ab}s_a s_b} + \frac{1}{J_{bb}s_b^2} \right), \quad (22)$$

$$\frac{1}{J^{(1)}} = \frac{1}{4} \left(\frac{1}{J_{aa}s_a} + \frac{1}{J_{bb}s_b} \right), \quad (23)$$

$$\frac{1}{J^{(2)}} = \frac{1}{4} \left(\frac{1}{J_{aa}} + \frac{1}{J_{bb}} \right). \quad (24)$$

Thus the NLSM action in the present case is given by Eq. (12) with Eqs. (22) to (24).

Substituting (22) and (23), the gapless equation (16) becomes

$$\frac{1}{J_{ab}} = \frac{1 - t_a(l)}{2t_b(l)} \frac{1}{J_{aa}} + \frac{1 - t_b(l)}{2t_b(l)} \frac{s_a}{s_b} \quad (25)$$

with

$$t_a(l) = \frac{2l - 1}{4s_a}, \quad t_b(l) = \frac{2l - 1}{4s_b} \quad (26)$$

in the unit of $J_{bb} = 1$. The gapless equation (25) represents a straight *gapless line* for each l in the plane of $(1/J_{aa}, 1/J_{ab})$. The part of a gapless line in the first quadrant is physical. For negative l , Eq. (25) does not produce a line which passes through the first quadrant. Hence we hereafter consider l as a positive integer.

When s_a and s_b are fixed, all the gapless lines with different values of l intersect at a single point

$$\left(-\frac{s_a}{s_b}, \frac{1}{2} \left(1 - \frac{s_a}{s_b} \right) \right). \quad (27)$$

We call it the *focus*; this is in the second quadrant. The slope of Eq. (25) monotonically decreases as l increases. The maximum slope is $2s_b(1 - 1/4s_a)$ for $l = 1$. For large l , gapless lines accumulate toward the line

$$\frac{1}{J_{ab}} = -\frac{s_b}{2s_a} \frac{1}{J_{aa}} - \frac{s_a}{2s_b}, \quad (28)$$

which is outside the first quadrant. The gapless lines for $l = 1, 2, \dots, 2s_b$ are physical, because they go through the first quadrant. The slope of a gapless line is positive if $1 \leq l \leq 2s_a$, and negative if $2s_a + 1 \leq l \leq 2s_b$. A gapless line with smaller l has a larger slope.

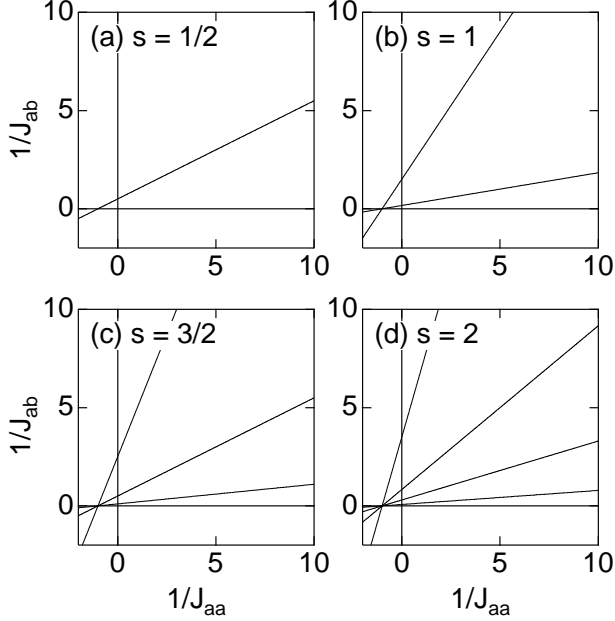


FIG. 2. Gapless lines for (a) $s = \frac{1}{2}$, (b) 1, (c) $\frac{3}{2}$ and (d) 2 in the case of $s_a = s_b (\equiv s)$. The unit of $J_{bb} = 1$ is used. The first quadrants represent the phase diagrams in the $1/J_{aa}$ - $1/J_{ab}$ plane. Phase boundaries are the gapless lines.

V. HOMOGENEOUS SPIN MAGNITUDE

In the case of $s_a = s_b \equiv s$, the spin magnitude is homogeneous and only the exchange coupling has a spatial modulation with period 4. Then the gapless equation (25) is reduced to

$$\frac{1}{J_{ab}} = -\frac{1}{2} \left(1 - \frac{4s}{2l-1} \right) \left(\frac{1}{J_{aa}} + 1 \right). \quad (29)$$

This equation gives gapless lines for $l = 1, 2, \dots, 2s$ for each s . Figure 2 shows them for $s = \frac{1}{2}, 1, \frac{3}{2}$ and 2 in the $1/J_{aa}$ - $1/J_{ab}$ plane. The focus is $(-1, 0)$ for all s and only the first quadrant is physical. These gapless lines determine the phase boundaries among disordered phases. The corresponding phase diagrams in the J_{aa} - J_{ab} plane are shown in Fig. 3. When we consider the uniform case ($J_{aa} = J_{ab} = 1 (= J_{bb})$), the gapless condition of Eq. (29) becomes $s = (2l - 1)/2$, the Haldane's original result [1].

In the simplest case of $s = \frac{1}{2}$, Eq. (29) has a physical solution ($J_{aa} > 0, J_{ab} > 0$) only for $l = 1$ as shown in Fig. 2(a) and Fig. 3(a). Chen and Hida performed numerical calculation in this case and obtained a phase boundary [14]. The gapless line given by the present NLSM method qualitatively agrees with their numerical phase boundary in the positive J_{ab} region [17].

The phases in Fig. 2 or 3 are interpreted by extending the valence-bond-solid (VBS) picture. In the original

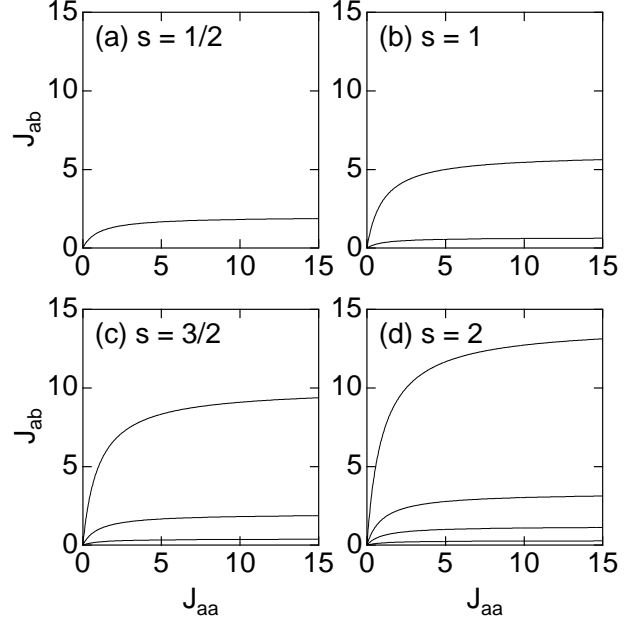


FIG. 3. Phase diagrams in the J_{aa} - J_{ab} plane for $s_a = s_b (\equiv s)$. The unit of $J_{bb} = 1$ is used.

VBS picture [12], a state with spin gap is represented by the direct product of singlet dimers. Chen and Hida [14] extended the VBS picture to include local singlet states each of which is formed by four $\frac{1}{2}$ -spins. Using the extended VBS picture they explained their numerical phases in the $s = \frac{1}{2}$ case. We call the local singlet state the *singlet cluster* or simply the cluster. We further extend the concept of the cluster to include a local singlet formed by more than four $\frac{1}{2}$ -spins; we will encounter larger clusters in the next section. We refer the direct product state of regularly arrayed clusters as the *singlet cluster solid* (SCS). We can explain the disordered phases for arbitrary s in the SCS picture.

For definiteness, we explain the case of $s = \frac{3}{2}$ in the SCS picture; the explanation for other values of s is almost the same. In Fig. 4 the $s = \frac{3}{2}$ spin at each site is decomposed into three $\frac{1}{2}$ -spins, which are represented by small circles. The symmetrization of the wave function for the $\frac{1}{2}$ -spins at a site retrieves the original $\frac{3}{2}$ -spin. A loop represents a local singlet state of two or four $\frac{1}{2}$ -spins in it, while a dotted line represents a spatially extended singlet state. Figures 4(a), (c), (e) and (g) illustrate clockwise the phases in the first quadrant of Fig. 2(c). We label them by $C(6), C(4, 1), C(2, 2)$ and $C(0, 3)$, respectively. For example, $C(6)$ means that there are 6 singlet dimers in a unit cell, while $C(4, 1)$ means that there are 4 singlet dimers and 1 singlet cluster formed by four $\frac{1}{2}$ -spins. Figures 4(b), (d) and (f) illustrate the states on the phase boundaries determined as the gapless lines with $l = 1, 2$ and 3, respectively.

We first examine the phase $C(6)$ above the gapless line

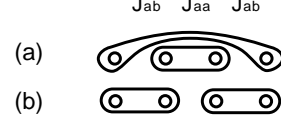


FIG. 5. Basis states (a) $|aa, bb\rangle$ and (b) $|ba, ab\rangle$ for a cluster of four $\frac{1}{2}$ -spins (Eq. (30)).

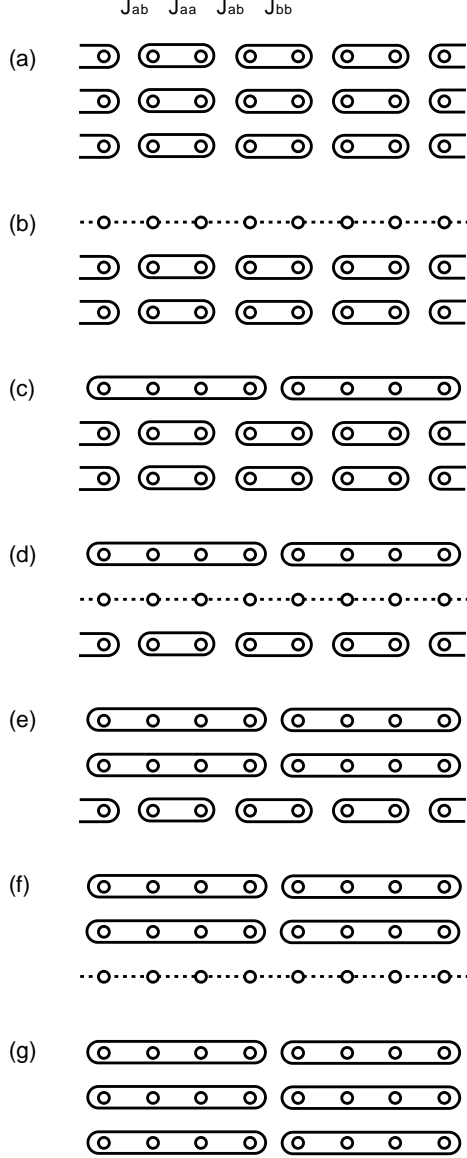


FIG. 4. The SCS picture for the phases in the case of $s = 3/2$ ($= s_a = s_b$). The SCS states are labeled by (a) $C(6)$, (c) $C(4, 1)$, (e) $C(2, 2)$ and (g) $C(0, 3)$.

of $l=1$ in Fig. 2(c), which corresponds to the narrow region just above the J_{aa} -axis in Fig. 3(c). In this phase, J_{ab} is much smaller than both J_{aa} and J_{bb} ($=1$). Hence the ground state in the phase is the VBS state as shown in Fig. 4(a), where singlet dimers are formed on J_{aa} - and J_{bb} -couplings. As J_{ab} increases, energy reduction by forming the dimers on the J_{aa} - and J_{bb} -couplings relatively decreases, since dimers on J_{ab} -couplings could reduce the energy. When J_{ab} arrives at a critical value, two singlet dimers per unit cell are broken and an extended state appears as shown in Fig. 4(b). The extended singlet state explains the gapless line with the largest slope ($l=1$) in Fig. 2(c).

When J_{ab} increases further, the $\frac{1}{2}$ -spins forming the spatially extended singlet state recombine to form singlet clusters of four $\frac{1}{2}$ -spins. Then the state becomes $C(4, 1)$ as shown in Fig. 4(c). The formation of the cluster partially gain the exchange energy on the J_{ab} -couplings as well as that on the J_{aa} -coupling. A singlet cluster of four $\frac{1}{2}$ -spins is a linear combination of two basis states:

$$|c^{(4)}\rangle = w_1 |aa, bb\rangle + w_2 |ba, ab\rangle. \quad (30)$$

Here $|aa, bb\rangle$ is the direct product of two singlet pairs in the cluster; one is a dimer pair of the adjacent s_a 's and the other is an extended pair of s_b 's as shown in Fig. 5(a). The state $|ba, ab\rangle$ is the direct product of two singlet dimers as shown in Fig. 5(b). The relative weight w_1/w_2 of the basis states changes continuously when the exchange parameters changes within this phase region. In contrast, the change from the state in Fig. 4(a) to that in Fig. 4(c) has occurred along with the disappearance of a series of singlet dimers and the appearance of a series of singlet clusters. Hence the system has experienced a phase transition between these two states. The critical state on the phase boundary is the gapless state in Fig. 4(b).

When J_{ab} increases further from the state of Fig. 4(c), we can repeat the same explanation. That is, a series of remnant singlet dimers are broken and singlet clusters increase as in Fig. 4(e) and finally as in Fig. 4(g). The gapless extended states in Figs. 4(d) and 4(f) appear as critical states in the way of changing. They correspond to phase boundaries in Fig. 2(c) and Fig. 3(c).

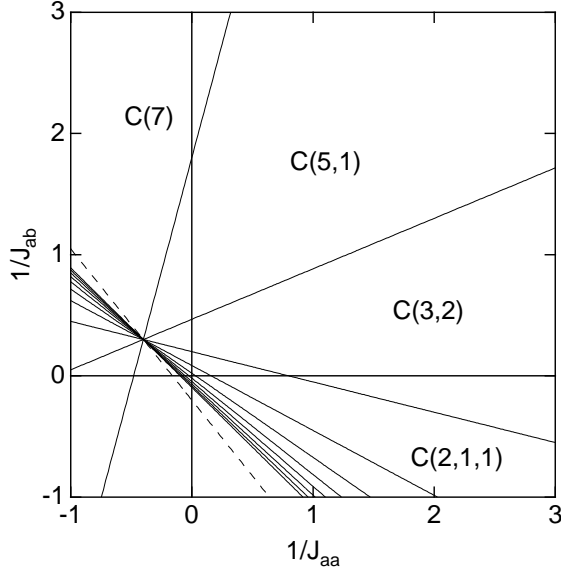


FIG. 6. Gapless lines for $s_a = 1$ and $s_b = 5/2$. The lines with $l \leq 10$ in Eq. (25) are displayed, but only the lines with $l \leq 5$ pass through the first quadrant. The dotted line is the large- l limit of Eq. (25). The first quadrant is the phase diagram in the $1/J_{aa}$ - $1/J_{ab}$ plane.

VI. INHOMOGENEOUS SPIN MAGNITUDE

We examine the phase diagram for $s_a < s_b$. The phase boundaries, i. e. gapless lines, are given by Eq. (25) for $l = 1, 2, \dots, 2s_b$.

The simplest example is the model with $s_a = \frac{1}{2}$ and $s_b = 1$. In a previous paper, we examined this case and presented the phase diagram in the NLSM method [18]. On the other hand, Tonegawa et al. [19] and Hikihara et al. [20] performed numerical calculation for the same case and obtained the numerical phase diagram. The overall feature of our phase diagram well agrees with that of the numerical one in this example.

As a typical example with general features, we explain the case of $s_a=1$ and $s_b=\frac{5}{2}$ in detail. The phase boundaries are given by Eq. (25) with $l = 1, 2, \dots, 5$. The phase diagram in the $1/J_{aa}$ - $1/J_{ab}$ plane is shown in Fig. 6, where only the first quadrant is physical. All the gapless lines intersect on the focus $(-\frac{2}{5}, \frac{3}{10})$ from Eq. (27) and accumulate to the line $J_{ab}^{-1} = -\frac{5}{4}J_{aa}^{-1} - \frac{1}{5}$ from Eq. (28). There are 6 phases in the first quadrant. We label them clockwise as $C(7)$, $C(5,1)$, $C(3,2)$, $C(2,1,1)$, $C(1,0,2)$ and $C(0,0,1,1)$; the last two are not indicated in Fig. 6 because of the lack of space. We will soon explain the general notation after introducing the SCS picture for the present example. The corresponding phase diagram in the J_{aa} - J_{ab} plane is shown in Fig. 7. We have taken the logarithms for J_{aa} and J_{ab} because of the largely different scales of the phases.

We interpret the gapful phases in the SCS picture. We

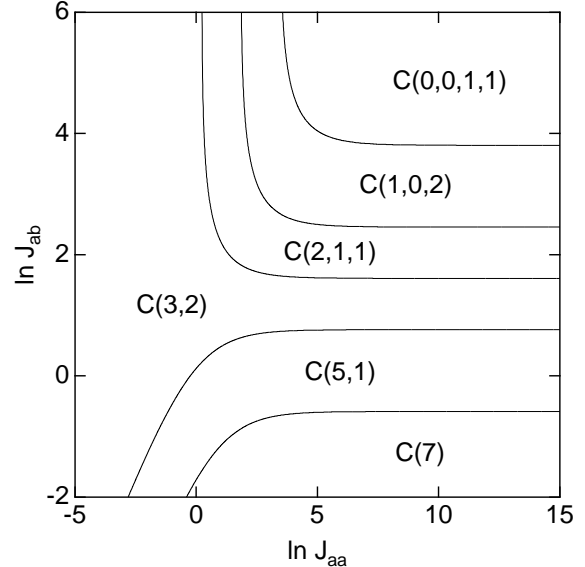


FIG. 7. Phase diagram for $s_a = 1$ and $s_b = 5/2$ in the J_{aa} - J_{ab} plane. Logarithm is taken for each axis.

first decompose the spin (with magnitude s_a or s_b) at each site into $\frac{1}{2}$ -spins in the same manner as in Sec. V. The original spin is retrieved by symmetrizing the wave function for the $\frac{1}{2}$ -spins at the same site. We represent a gapful phase as an SCS state, which is a direct product of singlet clusters. The SCS states for $s_a=1$ and $s_b=\frac{5}{2}$ are illustrated in Fig. 8. Each decomposed $\frac{1}{2}$ -spin is represented by a small circle. A loop containing an even number of $\frac{1}{2}$ -spins means a singlet cluster, while a dotted line means an extended singlet state. The general SCS state is labeled as

$$C(k_1, k_2, k_3, \dots), \quad (31)$$

where k_j is the number of singlet clusters formed by $2j$ $\frac{1}{2}$ -spins in a unit cell. SCS states of $C(k_1)$ and $C(k_1, k_2)$ have been introduced in Sec. V. For example, a unit cell of $C(0,0,1,1)$ includes a singlet cluster consisting of four $\frac{1}{2}$ -spins and a singlet cluster consisting of six $\frac{1}{2}$ -spins.

We explain the phases in the first quadrant of Fig. 6 clockwise starting from the phase $C(7)$. In this phase, J_{ab} is much smaller than both J_{aa} and J_{bb} ($=1$) so that a singlet dimer is not formed on any J_{ab} -coupling. Hence the $\frac{1}{2}$ -spins form singlet dimers on J_{aa} - and J_{bb} -couplings to gain exchange energies. This ground state is explained as a VBS state illustrated in Fig. 8(a). When J_{ab} increases, the system experiences the transitions from $C(7)$ to $C(5,1)$ and from $C(5,1)$ to $C(3,2)$. Then singlet dimers decrease and singlet clusters consisting of four $\frac{1}{2}$ -spins increase in each unit cell. The ground states of $C(5,1)$ and $C(3,2)$ are illustrated in, respectively, (c) and (e) of Fig. 8. The states in (b) and (d) are on the phase boundaries. Extended singlet states appear just when a series of singlet dimers are broken and a series of singlet

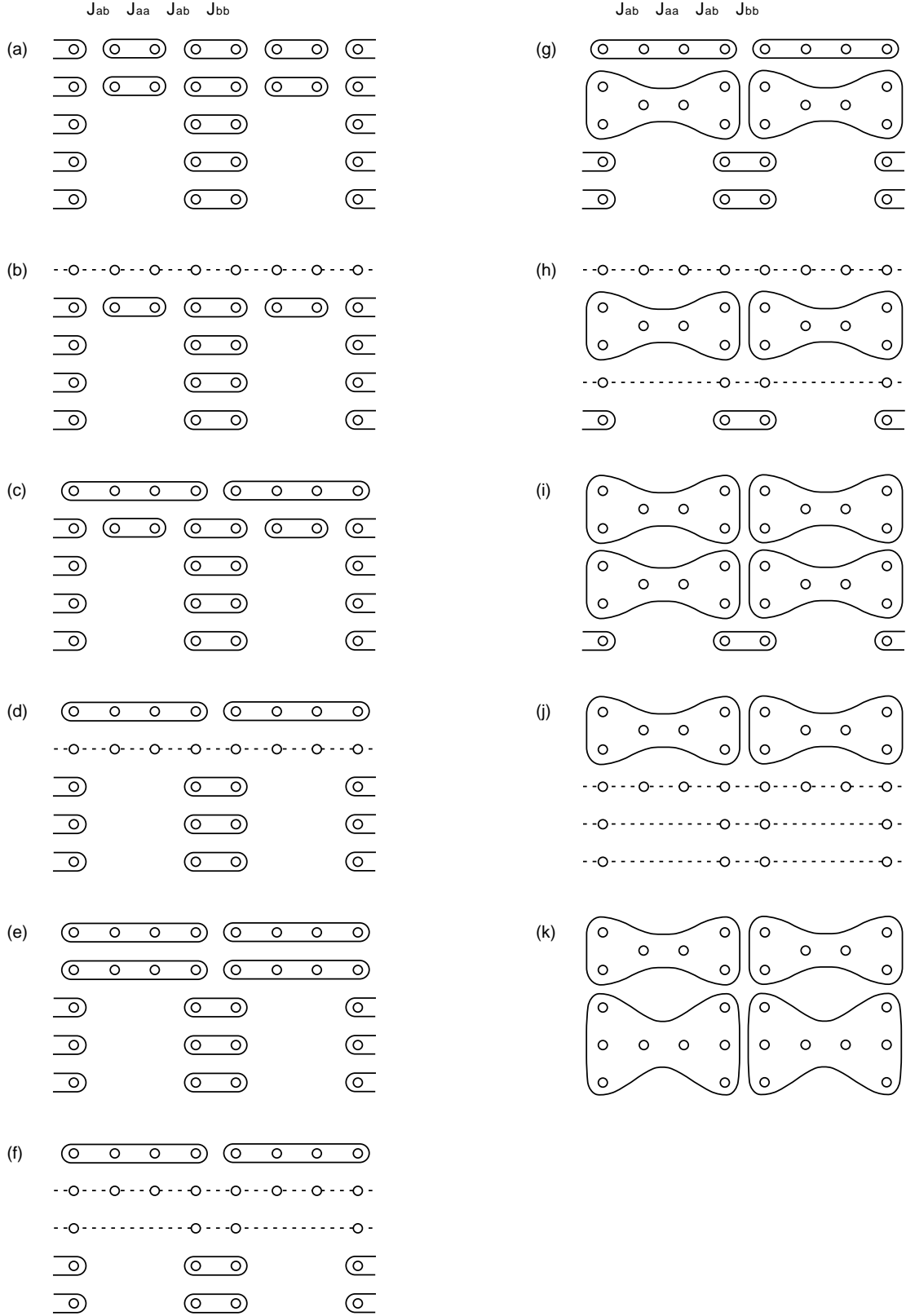


FIG. 8. The SCS picture for $s_a=1$ and $s_b=\frac{5}{2}$. Gapful phases in Fig. 6 or 7 are represented by (a) $C(7)$, (c) $C(5, 1)$, (e) $C(3, 2)$, (g) $C(2, 1, 1)$, (i) $C(1, 0, 2)$ and (k) $C(0, 0, 1, 1)$. The other figures represent gapless states on phase boundaries.

clusters are formed. Gapless spin excitations originate from the extended states. Until now the explanation is the same as that for the homogeneous case in Sec. V.

The region of $C(3, 2)$ in the J_{aa} - J_{ab} plane (Fig. 7) is T-shaped; the T is rotated by 90 degrees. We explain the origin of this shape by Fig. 8(e). A singlet cluster state of four $\frac{1}{2}$ -spins in this figure is described by Eq. (30). First, in the large J_{aa} part of this T-shaped region, J_{aa} is much larger than the others. Hence, in a cluster, the state $|aa, bb\rangle$ including a dimer on the J_{aa} -coupling is more favorable than $|ba, ab\rangle$; i. e. the weight w_1 is much larger than w_2 in Eq. (30). Second, in the large J_{ab} part of the T-shaped region, J_{ab} is larger than J_{aa} and J_{bb} ($=1$). Hence the state $|ba, ab\rangle$ is favorable since it consists of two singlet dimers on J_{ab} -couplings; i. e. the weight w_2 is much larger than w_1 . Third, in the small J_{ab} part of the T-shaped region, J_{bb} ($=1$) is larger than the others. Because of the lack of a J_{bb} -coupling within a cluster, there is no particularly favorable dimers in Eq. (30). The state $|aa, bb\rangle$ or $|ba, ab\rangle$ individually gains the exchange energy to some extent. However comparable values of w_1 and w_2 further reduce the total energy because of the off-diagonal matrix element $\langle aa, bb | H | ba, ab \rangle$. Thus the above three parts are differently characterized, but they belong to the same phase and merge around $(J_{aa}, J_{ab}) = (1, 1)$. One can move from one part to another by continuously changing the weights, w_1 and w_2 , with no phase transition.

When J_{aa} and J_{ab} become larger, the system further intends to gain the exchange energies on J_{aa} - and J_{ab} -couplings rather than on J_{bb} -couplings. Then the ground state $C(3, 2)$ changes into $C(2, 1, 1)$. In $C(2, 1, 1)$, singlet clusters consisting of six $\frac{1}{2}$ -spins appear as shown in Fig. 8(g). At the moment of the transition from $C(3, 2)$ to $C(2, 1, 1)$, a series of singlet dimers on J_{bb} -couplings break and an extended state appears as shown in Fig. 8(f). The gapless phase boundary in Fig. 6 and Fig. 7 results from the extended states. As J_{aa} and J_{ab} become further large, singlet dimers on J_{bb} -couplings become much more unfavorable for the energy reduction. Instead the system reduces the total energy by forming more or larger singlet clusters. Hence the ground states in Fig. 8(i) and (k) appear as both J_{aa} and J_{ab} increase. These ground states correspond to the phases $C(1, 0, 2)$ and $C(0, 0, 1, 1)$. There appear gapless extended states (h) and (j) of Fig. 8 at the transitions from (g) to (i) and from (i) to (k), respectively. They correspond to the phase boundaries between $C(2, 1, 1)$ and $C(1, 0, 2)$, and between $C(1, 0, 2)$ and $C(0, 0, 1, 1)$.

In the general case of arbitrary s_a and s_b ($s_a < s_b$), the number of phases may be large but the structure of the phase diagram is essentially the same. There are $2s_b + 1$ phases divided by $2s_b$ phase boundaries or gapless lines, which are given by Eq. (25) for $l = 1, 2, \dots, 2s_b$. The phase below the line of $l=1$ in the J_{aa} - J_{ab} plane is interpreted as a VBS state $C(2s_b + 2s_a)$ consisting only of singlet dimers like Fig. 8(a). As J_{ab} increases, the system successively undergoes the phases $C(2s_b + 2s_a - 2, 1)$,

$C(2s_b + 2s_a - 4, 2), \dots, C(2s_b - 2s_a, 2s_a)$. For each phase change, two singlet dimers disappear and a cluster with four $\frac{1}{2}$ -spins appears in each unit cell. The $(2s_a + 1)$ th phase $C(2s_b - 2s_a, 2s_a)$ is T-shaped like $C(3, 2)$ of Fig. 7. As J_{ab} further increases with J_{aa} , the number of the singlet dimers continues to decrease one by one; for a single phase change a singlet dimer disappears and a larger cluster with more than four $\frac{1}{2}$ -spins is formed in each unit cell. Hence there are $2s_b - 2s_a$ phases above the boundary line of $l = 2s_a + 1$ in the J_{aa} - J_{ab} plane. In the phase of the large limit of J_{ab} , there are $2s_a$ clusters like Fig. 8(k). Hence a cluster in this phase includes $2(s_a + s_b)/s_a$ $\frac{1}{2}$ -spins in average. That is, there are clusters with $[2s_b/s_a] + 2$ $\frac{1}{2}$ -spins and clusters with $[2s_b/s_a] + 3$ $\frac{1}{2}$ -spins; here $[\dots]$ means the integer part of the number inside. Thus we have explained the $2s_b$ phase transitions which appear with increasing J_{ab} (and J_{aa}).

VII. SUMMARY AND DISCUSSION

We applied the previously developed NLSM method to the mixed spin chain consisting of spins with magnitudes s_a and s_b ($s_a \leq s_b$). They are arrayed as s_a - s_a - s_b - s_b and the exchange parameters are periodic with period 4. The NLSM for this spin chain yields the gapless equation which determines the $2s_b$ phase boundaries. Thus we obtained the phase diagram in the exchange parameter space. The number of the phases is $2s_b + 1$ irrespective of s_a . To explain the ground states in the phase diagram we proposed the SCS picture, which is an extension of the VBS picture. In the SCS picture, the gapful ground state in each phase is represented as a direct product of regularly arrayed singlet clusters. Then the phase transition is a change from an SCS state to another and a gapless state appears just at the change. The SCS picture qualitatively explains, in a unified way, all the phases which were obtained by the present NLSM method for arbitrary s_a and s_b .

The phase diagrams for simple cases were compared to results of numerical calculations. The features of the phase boundaries qualitatively agree with those of the numerical calculations for $s_a = s_b = \frac{1}{2}$ [10, 14] and for $s_a = \frac{1}{2}$ and $s_b = 1$ [18–20]. It is expected that numerical calculations will be performed for various s_a and s_b . Experiments for real materials have not been seen yet. It is also expected that materials with various s_a and s_b will be found and experiments will be performed for them.

ACKNOWLEDGMENT

I thank Kazuo Hida for useful discussion. This work is supported by the Grant-in-Aid for Scientific Research from the Ministry of Education, Science, Sports and Culture, Japan.

-
- [1] F. D. M. Haldane, Phys. Lett. **93A**, 464 (1983); Phys. Rev. Lett. **50**, 1153 (1983).
- [2] I. Affleck, "Field Theory Methods and Quantum Critical Phenomena" in *Fields, Strings and Critical Phenomena*, Les Houches 1988, eds. E. Brezin and J. Zinn-Justin, North-Holland, 1990.
- [3] E. Fradkin, *Field Theories of Condensed Matter Physics*, Addison-Wesley Publishing, 1994.
- [4] A. M. Tsvelick, *Quantum Field Theories in Condensed Matter Physics*, Cambridge University Press, 1995.
- [5] I. Affleck, Nucl. Phys. B **257**, 397 (1985); **265**, 409 (1986).
- [6] I. Affleck and F. D. M. Haldane, Phys. Rev. **B36**, 5291 (1987).
- [7] Y. Kato and A. Tanaka, J. Phys. Soc. Jpn. **63**, 1277 (1994).
- [8] S. Yamamoto, J. Phys. Soc. Jpn. **63**, 4327 (1994).
- [9] M. Hagiwara, Y. Narumi, K. Kindo, M. Kohno, H. Nakano, R. Sato, and M. Takahashi, Phys. Rev. Lett. **80**, 1312 (1998).
- [10] K. Takano, Phys. Rev. Lett. **82**, 5124 (1999).
- [11] Fukui and Kawakami proposed another NLSM method for special inhomogeneous spin chains including the period-4 case: Phys. Rev. **B55**, 14709 (1997); Phys. Rev. **B56**, 8799 (1997). The difference between their method and the present is mentioned in Ref. [10].
- [12] I. Affleck, T. Kennedy, E. H. Lieb and H. Tasaki, Phys. Rev. Lett. **59**, 799 (1987).
- [13] K. Takano, K. Kubo and H. Sakamoto, J. Phys.: Condens. Matter **8**, 6405 (1996).
- [14] W. Chen and K. Hida, J. Phys. Soc. Jpn. **67**, 2910 (1998).
- [15] E. Lieb and D. Mattis, J. Math. Phys. **3**, 749 (1962).
- [16] The block must be taken as an even number of unit cells if a unit cell consists of an odd number of spins.
- [17] They parameterized the exchange parameters as $J_{aa} \equiv 1 - \delta$, $J_{bb} \equiv 1 + \delta$ and $J_{ab} \equiv j$. Then the equation (29) with $s = \frac{1}{2}$ and $l = 1$ reduces to $\delta = (1 - j)^{1/2}$. This equation and their numerical result are compared in a figure of their paper [14].
- [18] K. Takano, cond-mat/9909440.
- [19] T. Tonegawa, T. Hikihara, M. Kaburagi, T. Nishino, S. Miyashita and H.-J. Mikeska, J. Phys. Soc. Jpn. **67**, 1000 (1998).
- [20] T. Hikihara, T. Tonegawa, M. Kaburagi, T. Nishino, S. Miyashita and H.-J. Mikeska, unpublished.